Raman spectroscopy of substrate-induced compression and substrate doping in thermally cycled graphene

Chun-Chung Chen, Wenzhong Bao, Chia-Chi Chang, Zeng Zhao, Chun Ning Lau, and Stephen B. Cronin

Phys. Rev. B **85**, 035431 — Published 20 January 2012

DOI: 10.1103/PhysRevB.85.035431

Raman Spectroscopy of Substrate-Induced Compression and Substrate Doping in Thermally Cycled Graphene

Chun-Chung Chen[1], Wenzhong Bao[3], Chia-Chi Chang[2], Zeng Zhao[3], Chun Ning Lau[3], and Stephen B. Cronin[1]

[1]*Department of Electrical Engineering, University of Southern California, Los Angeles, CA 90089*

[2]*Department of Physics, University of Southern California, Los Angeles, CA 90089*

[3]*Department of Physics and Astronomy, University of California, Riverside, Riverside, CA 92521*

Abstract

By thermally cycling single layer graphene in air, we observe irreversible upshifts of the Raman *G* and *2D* bands of 24 cm^{-1} and 23 cm^{-1}, respectively. These upshifts are attributed to an in-plane compression of the graphene induced by the mismatch of thermal expansion coefficients between the graphene and the underlying Si/SiO_2 substrate, as well as doping effects from the trapped surface charge in the underlying substrate. Since the *G* and the *2D* band frequencies have different responses to doping, we can separate the effects of compression and doping associated with thermal cycling. By performing the thermal cycling in an argon gas environment and by comparing suspended and on-substrate regions of the graphene, we can separate the effects of gas doping and doping from the underlying substrate. Variations in the ratio of the *2D* to *G* band Raman intensities provide an independent measure of the doping in graphene that occurs during thermal cycling. During subsequent thermal cycles, both the *G* and *2D* bands downshift linearly with increasing temperature, and then upshift reversibly to their original frequencies after cooling. This indicates that no further compression or doping is

induced after the first thermal cycle. The observation of ripple formation in suspended graphene after thermal cycling confirms the induction of in-plane compression. The amplitude and wavelength of these ripples remain unchanged after subsequent thermal cycling, corroborating that no further compression is induced after the first thermal cycle.

In the study of graphene, Raman spectroscopy is used widely for identifying the thickness, carrier concentration, temperature, and strain[1-4]. The sensitivity of the Raman *G* and *2D* bands to both anharmonic coupling of phonon modes and carbon-carbon length make Raman spectroscopy a useful tool for studying the temperature and strain dependence of graphene[5-8]. Recently, Late *et al.* investigated the Raman spectra of single layer graphene on Si/SiO_2 substrates from 77K to 573K, and calibrated the temperature coefficient of the *G* and *2D* band Raman modes to be $\partial\omega_G/\partial T = -0.016$ cm^{-1}/K and $\partial\omega_{2D}/\partial T = -0.026$ cm^{-1}/K[9]. Abdula *et al.* have also reported temperature coefficients of $\partial\omega_G/\partial T = -0.035$ cm^{-1}/K and $\partial\omega_{2D}/\partial T = -0.07$ cm^{-1}/K for single layer graphene[10], which are significantly different from those of Late *et al*. Changes in the Raman *G* and *2D* bands are also used to estimate the effect of strain in graphene[11-14]. Mohiuddin *et al.* have observed strain-induced shifts in the Raman *G* and *2D* bands of graphene of $\partial\omega_G/\partial\varepsilon = -58$ $cm^{-1}/\%$ and $\partial\omega_{2D}/\partial\varepsilon = -144$ $cm^{-1}/\%$ for graphene under biaxial strain[15]. Ni *et al.* have reported $\partial\omega_G/\partial\varepsilon = -14.2$ $cm^{-1}/\%$ and $\partial\omega_{2D}/\partial\varepsilon = -27.8$ $cm^{-1}/\%$ of Raman *G* and *2D* bands shifts on graphene under uniaxial strain[6]. In addition to temperature and strain, doping also causes changes in the Raman spectra[16]. By applying a top gate voltage to single layer graphene, Das *et al.* observed a reduction in the intensity ratio of the 2*D* band to *G* band. They also observed *G* band frequency upshifts with both *n*- and *p*-type doping, while the *2D* band frequency upshifts with *p*-type dopingand downshifts with *n*-type doping[17].

While the temperature and strain coefficients of graphene Raman spectra have been reported in many previous works, the effects of strain and doping induced by the underlying substrate are usually not taken into consideration when estimating the Raman

temperature coefficient. However, graphene's negative thermal expansion coefficient[18-20] causes a geometric mismatch with most supporting substrates. In addition, graphene is often observed to be doped when the ambient temperature is varied [21], which implies that the effects of strain and doping cannot be neglected when calibrating the temperature coefficient of the Raman modes of graphene. In this work, we measure the Raman spectra of both suspended and supported graphene before, during, and after thermal cycling from 300K to 700K. Both the Raman *G* and *2D* bands are studied systematically. Atomic force microscopy (AFM) is used to determine the suspended graphene profile variation before and after thermal cycling. Thermal cycling in air and Ar gas environments enables us to indentify changes associated with gas doping. In doing so, we are able to separate the effects of doping, compression, and temperature in graphene through the interpretation of the resulting Raman spectra.

In this work, graphene flakes are deposited on Si/SiO_2 substrates using mechanical exfoliation[22, 23]. The number of graphene layers are identified using Raman spectroscopy by curve fitting the *2D* band[24-26]. Figures 1a and 1b show an optical microscope image and the Raman spectrum of a single layer graphene flake sample (SLG1) deposited on a Si/SiO_2 substrate. Thermal cycling from 300K to 700K and then back to 300K is performed in air using a Linkam THMS temperature controlled stage, while Raman spectra are taken during the thermal cycling process. The Raman spectra are collected by using a Renishaw spectrometer with a 532 nm laser focused in a 0.5 μm spot through a Leica microscope with a 100X objective lens. The laser power was kept low at 0.3 mW during the experiment. The influence of locally heating from the laser is believed to be negligible, since no temperature-induced downshifts of the *G* band

was observed, even when the laser power was increased from 0.3 mW to 1.5 mW. Raman data taken with different laser powers is presented in the online supplement document[27].

The *G* band and *2D* band Raman spectra of the single layer graphene sample (SLG1) taken during thermal cycling are shown in Figures 2a and 2b. During heating, the *G* band Raman shift remains approximately constant while the *2D* band downshifts monotonically. Since the *G* band is sensitive to both temperature and doping, the temperature-induced downshift[28] is approximately canceled by the effect doping, which upshifts the mode. The *2D* band frequency, on the other hand, has different response to doping, and exhibits the expected temperature-induced downshift. During cooling, linear upshifts are observed in both the *G* and *2D* bands, with temperature coefficients of $\partial\omega_G/\partial T = -0.057$ cm^{-1}/K and $\partial\omega_{2D}/\partial T = -0.092$ cm^{-1}/K, which are slightly higher than those observed in previous works [9, 10, 29]. By comparing the *G* and *2D* band Raman modes before and after thermal cycling (at 300K), the *G* band exhibits an irreversible upshift of 24.4 cm^{-1}, while the *2D* band upshifts by 23.2 cm^{-1}. This *G* band upshift is consistent with our previous work on suspended graphene, which showed a 25 cm^{-1} upshift in the supported region, while the suspended region remained constant after thermal cycling[30]. In this previous work, ripple formation in the suspended region of the graphene indicated that the *G* band upshift originated from the compression of the graphene lattice created by the mismatch of thermal expansion coefficients between the graphene and the underlying Si/SiO_2 substrate[18, 19, 31, 32]. In addition to compression, doping effects can also cause the *G* and *2D* bands upshifts. Das *et al*. have reported *G* band upshifts of 25 cm^{-1} and 7cm^{-1} linewidth narrowing due to

electrostatic doping, while the *2D* band upshifts by only 15 cm^{-1} for *p*-type and downshifts by 20 cm^{-1} for *n*-type doping[17]. In the experiment presented here, both *G* and *2D* bands show similar irreversible upshifts, while the *G* band FWHM narrowing is less than 2 cm^{-1} after thermal cycling. These results indicate that, in addition to substrate-induced doping effects, a significant amount of compression is created.

A second thermal cycle was carried out on the same sample (SLG1) to 700K and back to 300K. The Raman *G* and *2D* bands taken during the second thermal cycling are shown in Figures 3a and 3b. In the second thermal cycle, both the Raman *G* and *2D* bands downshift linearly with increasing temperature and upshift linearly to their original frequencies reversibly after cooling to 300K. Here, we observe Raman temperature coefficients of $\partial\omega_G/\partial T = -0.055$ cm^{-1}/K and $\partial\omega_{2D}/\partial T = -0.083$ cm^{-1}/K. It is important to note that no irreversible upshifts or downshifts of the *G* or *2D* bands are observed after the second thermal cycling. This implies that no further compression or doping has occurred in the graphene, and that these coefficients represent the *true* temperature dependence of the *G* and *2D* bands. Many previous works have measured the temperature coefficients of graphene[9, 10, 29], however the temperature coefficient reported from the previous works are not consistent with each other and span a wide range from -0.016 cm^{-1}/K to -0.035 cm^{-1}/K for the *G* band frequency. If we use our initial "heating" data in Figure 2(a) of the manuscript, we obtain comparable values to those in the literature, -0.034 cm^{-1}/K. However, the Raman spectra observed before and after thermal cycling exhibit irreversible upshifts of the *G* band after the thermal cycle is complete, which must be taken into consideration when estimating the temperature coefficients of graphene. Both heating and cooling processes are discussed in our experiment. After the thermal

cycling, we identify the substrate-induced compression and doping effects, which cause the large irreversible upshifts of the *G* band. These irreversible upshifts are included in our estimation of the temperature coefficients. Furthermore, the temperature coefficients established in this way are repeatable within the temperature range of the thermal cycling and are observed consistently during subsequent heating and cooling process.

In order to confirm the assumption that no further compression is induced in the graphene after the first thermal cycle, a triple layer graphene (TLG) flake suspended across a 3μm trench, shown in Figure 4c, was thermally cycled twice to 700K, while observing its Raman spectra. Figure 4a shows the height profiles of the suspended TLG measured by atomic force microscopy before and after the first thermal cycling, which exhibits uniform and periodic ripples after the first thermal cycle, indicative of compression. Spatially mapped *G* band shift taken before and after the first thermal cycle are shown in Figure 4b. *G* band upshifts of $9cm^{-1}$ and $4cm^{-1}$ are observed in the supported and suspended regions, respectively. The magnitude of these shifts are consistent with our previous work obtained for triple layer graphene.

After a second thermal cycle to 700K, this TLG sample exhibited only slight variations in the amplitude and wavelength of the ripples and in the spatially-mapped Raman spectra, as shown in Figures 5a and 5b. The consistency of these results before and after the second thermal cycling confirms that no further compression or doping are induced after the first thermal cycle.

We also measured the effect of sequential thermal cycling to incrementally higher temperatures. Another single layer graphene sample (SLG2) was first thermally cycled to 500K, then to 600K, and then to 700K. Figures 6a and 6b show the *G* and *2D* band

Raman data taken during these three thermal cycles. For the first thermal cycle to 500K, the *G* band shows an initial upshift during the heating process, while the *2D* band does not. This phenomenon can be attributed to the doping effect from the surrounding air and H_2O molecules attaching to the graphene surface. In addition, the amorphous SiO_2, which contains a significant density of surface states, can donate electrons to the graphene layer in order to balance the chemical potential of the graphene-SiO_2 interface [21]. In Figure 6, the room temperature positions of both the *G* and *2D* bands are observed to upshift after every subsequent thermal cycle. After the third thermal cycle to 700K, net upshifts of 25 cm^{-1} for the *G* band and 27 cm^{-1} for the *2D* band are observed, which are consistent with the upshifts of sample SLG1 shown in Figure 1a after a single thermal cycling to 700K. This observation confirms that the equilibrium between the graphene and the underlying Si/SiO_2 substrate is not broken until the graphene is taken to a higher temperature. For this sample, the Raman temperature coefficients of the *G* and *2D* bands are $\partial\omega_G/\partial T = -0.055$ cm^{-1}/K and $\partial\omega_{2D}/\partial T = -0.085$ cm^{-1}/K during the third cooling process, which are also consistent with the previous results.

In this work, we attribute the irreversible upshifts observed in the Raman spectra to in-plane compression and doping effects in the graphene[33, 34]. The in-plane compression effects can also be studied through the observation of ripple formation in suspended graphene, and the doping level in SLG samples can be studied by observing the Raman intensity ratio of the *2D* and *G* bands (I_{2D}/I_G). This intensity ratio reduces with increasing carrier concentration[35, 36]. Malard *et al.* have also thermally cycled on-substrate single layer graphene to 515K in Ar. In their experiment, no significant *2D* band upshifts were observed, and all *G* band upshifts and I_{2D}/I_G Raman intensity ratio changes

were attributed to doping alone[37]. Figure 7 shows the intensity ratio of the *2D* and *G* bands of SLG1 sample shown in Figures 1 and 2 taken during the first and second thermal cycles. This data indicates that the doping effects from the surrounding air molecules and underlying substrate cause a factor of 5 reduction in the relative intensity of the *2D* band after the first thermal cycle, while the variation of the intensity ratio after the second thermal cycle is negligible. These results imply that the SLG1 sample is doped during the first thermal cycle only[17, 38]. However, Malard *et al*. did not observe any significant upshifts in the *2D* band Raman mode in their thermally cycled graphene. In our work, on the other hand, both Raman *G* and *2D* bands upshifted after thermal cycling. The Raman *2D* band upshifts further confirm the substrate-induced compression on graphene, since graphene is *n*-type doped after annealed in vacuum, as reported by Romero, *et al*, and substrate-induced (*n*-type) doping would result in a *2D* band downshift [17, 21]. Therefore, the large *2D* band upshifts observed in this work indicate that substrate-induced compression plays a significant role in thermally cycled graphene.

In order to further investigate the effects of doping, a fresh single layer graphene sample (SLG3) was thermally cycled to 700K in an Ar gas environment to reduce the effect of gas doping, while the Raman spectra are monitored. The Raman data of sample SLG3 (not shown) measured in Ar shows that during the cooling process the Raman temperature coefficients, $\partial\omega_G/\partial T = -0.048$ cm^{-1}/K and $\partial\omega_{2D}/\partial T = -0.080$ cm^{-1}/K, are slightly reduced compared with that in air. Both the *G* and *2D* bands still show large irreversible upshifts (21.2 cm^{-1} and 27.1 cm^{-1}) after thermal cycling in Ar. These results prove that the large upshifts observed in both air and Ar are dominated by compression and doping induced by the underlying substrate.

Table 1 shows a summary of the Raman data of three different single layer graphene samples after thermal cycling to 700K. In this table, the SLG1 and SLG2 samples show similar temperature coefficients and *G* and *2D* band upshifts, even though SLG2 has been cycled sequentially to 500K, 600K, and then 700K. The temperature coefficient of SLG3 is slightly lower than that of SLG1 and SLG2. The lower I_{2D}/I_G variation of SLG3 after 700K thermal cycling indicates that the gas doping effect is reduced by the Ar atmosphere.

In conclusion, *G* band and *2D* band upshifts of 24 cm^{-1} and 23 cm^{-1} were observed after thermal cycling single layer graphene to 700K. These upshifts are attributed to the compression of the graphene induced from the underlying SiO_2/Si substrate and doping effects from the trapped charges in the underlying substrate. No irreversible upshifts were observed after a second thermal cycle to 700K, indicating that no further compression or doping is induced after the first thermal cycle. By separating the effects of doping, compression, and temperature in graphene, through the interpretation of the resulting Raman spectra, we are able to determine the true temperature dependence of the *G* and *2D* bands. Repeatable Raman temperature coefficients are observed after the first thermal cycle, giving SLG Raman temperature coefficients of the *G* and *2D* bands of $\partial\omega_G/\partial T$ = -0.055 cm^{-1}/K and $\partial\omega_{2D}/\partial T$ = -0.085 cm^{-1}/K, respectively. These results provide a more complete understanding of the graphene-substrate interaction, which can result in significant variations of graphene's electrical, mechanical, and optical properties.

Acknowledgements

This research was supported in part by DOE Award No. DE-FG02-07ER46376, ONR Award No. N000141010511, and NSF award No. CBET-0854118.

References

1. Calizo, I., et al., *Temperature dependence of the Raman spectra of graphene and graphene multilayers.* Nano Letters, 2007. **7**(9): p. 2645-2649.
2. Calizo, I., et al., *Variable temperature Raman microscopy as a nanometrology tool for graphene layers and graphene-based devices.* Applied Physics Letters, 2007. **91**(7): p. 071913.
3. Allen, M.J., et al., *Temperature dependent Raman spectroscopy of chemically derived graphene.* Applied Physics Letters, 2008. **93**(19): p. 193119.
4. Calizo, I., et al., *Raman nanometrology of graphene: Temperature and substrate effects.* Solid State Communications, 2009. **149**(27-28): p. 1132-1135.
5. Ci, L.J., et al., *Temperature dependence of resonant Raman scattering in double-wall carbon nanotubes.* Applied Physics Letters, 2003. **82**(18): p. 3098-3100.
6. Ni, Z.H., et al., *Uniaxial Strain on Graphene: Raman Spectroscopy Study and Band-Gap Opening* ACS Nano, 2009. **3**(2): p. 483-483.
7. Lin, J.J., et al., *Anharmonic phonon effects in Raman spectra of unsupported vertical graphene sheets.* Physical Review B, 2011. **83**(12).
8. Chang, C.C., et al., *A New Lower Limit for the Ultimate Breaking Strain of Carbon Nanotubes.* ACS Nano, 2010. **4**(9): p. 5095-5100.
9. Late, D.J., et al., *Temperature effects on the Raman spectra of graphenes: dependence on the number of layers and doping.* Journal of Physics-Condensed Matter, 2011. **23**(5): p. 055303.
10. Abdula, D., et al., *Environment-Induced Effects on the Temperature Dependence of Raman Spectra of Single-Layer Graphene.* Journal of Physical Chemistry C, 2008. **112**(51): p. 20131-20134.
11. Yu, T., et al., *Raman mapping investigation of graphene on transparent flexible substrate: The strain effect.* Journal of Physical Chemistry C, 2008. **112**(33): p. 12602-12605.
12. Huang, M.Y., et al., *Probing Strain-Induced Electronic Structure Change in Graphene by Raman Spectroscopy.* Nano Letters, 2010. **10**(10): p. 4074-4079.
13. Huang, M.Y., et al., *Phonon softening and crystallographic orientation of strained graphene studied by Raman spectroscopy.* Proceedings of the National Academy of Sciences of the United States of America, 2009. **106**(18): p. 7304-7308.
14. Ferralis, N., *Probing mechanical properties of graphene with Raman spectroscopy.* Journal of Materials Science, 2010. **45**(19): p. 5135-5149.
15. Mohiuddin, T.M.G., et al., *Uniaxial strain in graphene by Raman spectroscopy: G peak splitting, Gruneisen parameters, and sample orientation.* Physical Review B, 2009. **79**(20): p. 205433.
16. Ferrari, A.C., *Raman spectroscopy of graphene and graphite: Disorder, electron-phonon coupling, doping and nonadiabatic effects.* Solid State Communications, 2007. **143**(1-2): p. 47-57.
17. Das, A., et al., *Monitoring dopants by Raman scattering in an electrochemically top-gated graphene transistor.* Nature Nanotechnology, 2008. **3**(4): p. 210-215.

18. Mounet, N. and N. Marzari, *First-principles determination of the structural, vibrational and thermodynamic properties of diamond, graphite, and derivatives.* Physical Review B, 2005. **71**(20): p. 205214.
19. Singh, V., et al., *Probing thermal expansion of graphene and modal dispersion at low-temperature using graphene nanoelectromechanical systems resonators.* Nanotechnology, 2010. **21**(16): p. 209801.
20. Bao, W.Z., et al., *Controlled ripple texturing of suspended graphene and ultrathin graphite membranes.* Nature Nanotechnology, 2009. **4**(9): p. 562-566.
21. Romero, H.E., et al., *n-Type Behavior of Graphene Supported on Si/SiO_2 Substrates.* ACS Nano, 2008. **2**(10): p. 2037-2044.
22. Novoselov, K.S., et al., *Electronic properties of graphene.* Physica Status Solidi B-Basic Solid State Physics, 2007. **244**(11): p. 4106-4111.
23. Castro Neto, A.H., et al., *The electronic properties of graphene.* Reviews of Modern Physics, 2009. **81**(1): p. 109-162.
24. Gupta, A., et al., *Raman scattering from high-frequency phonons in supported n-graphene layer films.* Nano Letters, 2006. **6**(12): p. 2667-2673.
25. Ferrari, A.C., et al., *Raman spectrum of graphene and graphene layers.* Physical Review Letters, 2006. **97**(18): p. 187401.
26. Malard, L.M., et al., *Raman spectroscopy in graphene.* Physics Reports-Review Section of Physics Letters, 2009. **473**(5-6): p. 51-87.
27. *See Supplemental Material at for Raman data taken with different laser power.*
28. Haiqing Zhou, C.Q., Fang Yu, Huaichao Yang, Minjiang Chen, Lijun Hu, Yanjun Guo and Lianfeng Sun, *Raman scattering of monolayer graphene: the temperature and oxygen doping effects.* Journal of Physics D: Applied Physics, 2011. **44**(18): p. 185404.
29. Zhang, L., et al., *Low-temperature Raman spectroscopy of individual single-wall carbon nanotubes and single-layer graphene.* Journal of Physical Chemistry C, 2008. **112**(36): p. 13893-13900.
30. Chen, C.C., et al., *Raman Spectroscopy of Ripple Formation in Suspended Graphene.* Nano Letters, 2009. **9**(12): p. 4172-4176.
31. Tada, H., et al., *Thermal expansion coefficient of polycrystalline silicon and silicon dioxide thin films at high temperatures.* Journal of Applied Physics, 2000. **87**(9): p. 4189-4193.
32. Watanabe, H., N. Yamada, and M. Okaji, *Linear thermal expansion coefficient of silicon from 293 to 1000 K.* International Journal of Thermophysics, 2004. **25**(1): p. 221-236.
33. Yan, J., et al., *Electric field effect tuning of electron-phonon coupling in graphene.* Physical Review Letters, 2007. **98**(16): p. 166802.
34. Stampfer, C., et al., *Raman imaging of doping domains in graphene on SiO2.* Applied Physics Letters, 2007. **91**(24): p. 241907.
35. Basko, D.M., S. Piscanec, and A.C. Ferrari, *Electron-electron interactions and doping dependence of the two-phonon Raman intensity in graphene.* Physical Review B, 2009. **80**(16): p. 165408.
36. Berciaud, S., et al., *Probing the Intrinsic Properties of Exfoliated Graphene: Raman Spectroscopy of Free-Standing Monolayers.* Nano Letters, 2009. **9**(1): p. 346-352.

37. Malard, L.M., et al., *Thermal enhancement of chemical doping in graphene: a Raman spectroscopy study.* Journal of Physics-Condensed Matter, 2010. **22**(33): p. 334202.
38. Casiraghi, C., *Doping dependence of the Raman peaks intensity of graphene close to the Dirac point.* Physical Review B, 2009. **80**(23): p. 233407.

Figures

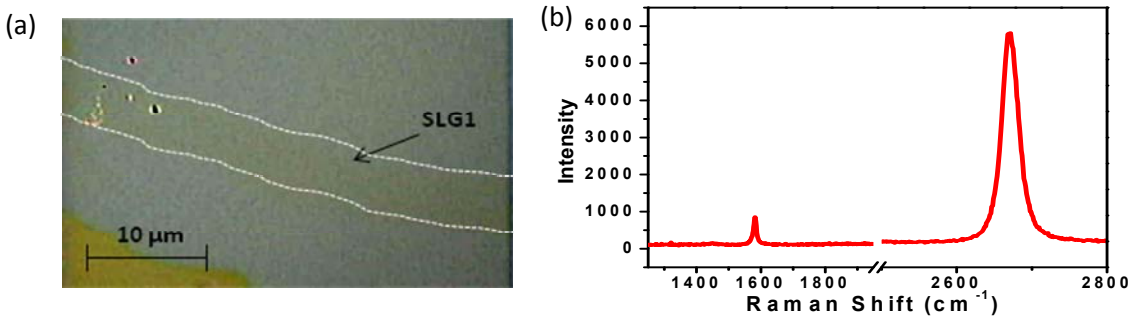

Figure 1. (a) Optical image of single layer graphene (SLG1) and (b) Raman spectrum of SLG1.

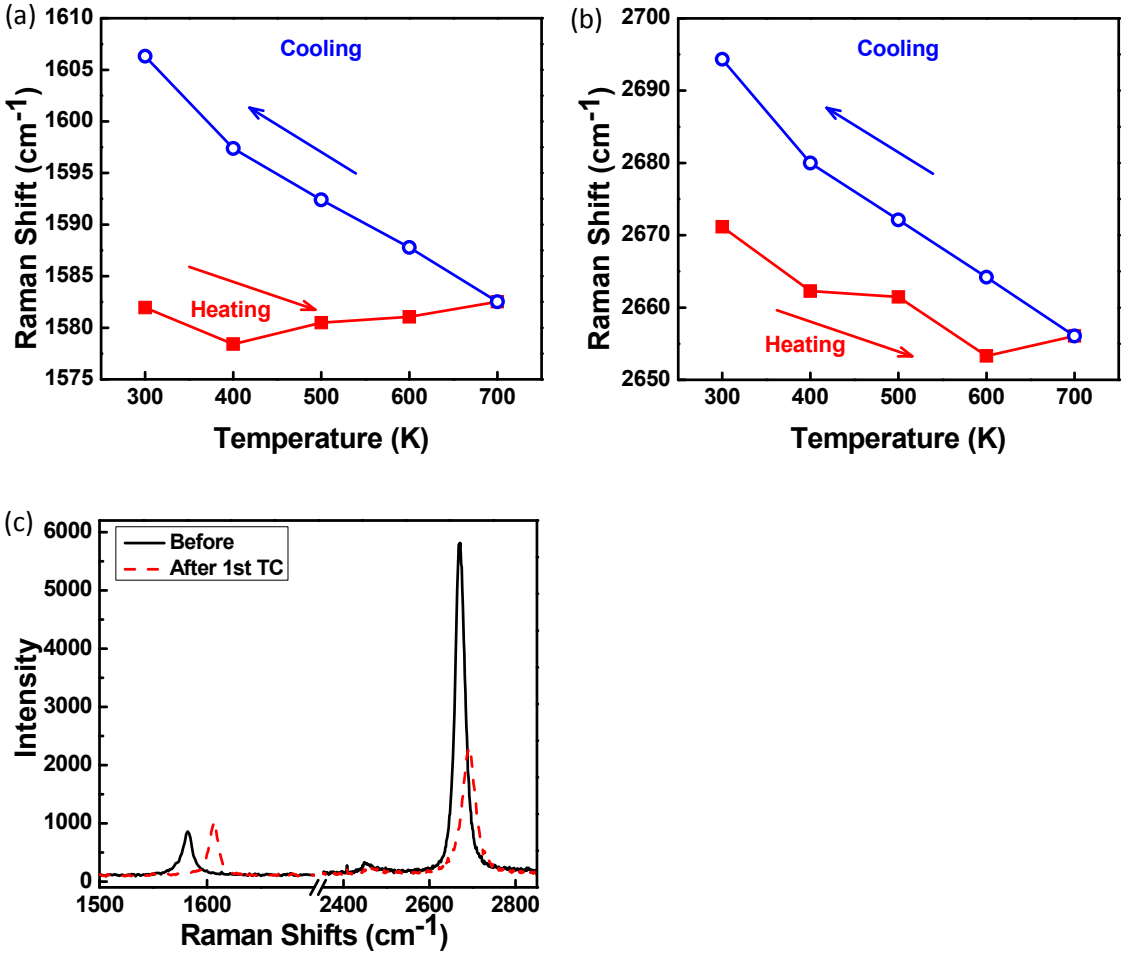

Figure 2. (a) *G* band and (b) *2D* band Raman data of single layer graphene taken during the first thermal cycling. (c) Raman spectrum before and after the first thermal cycling (TC).

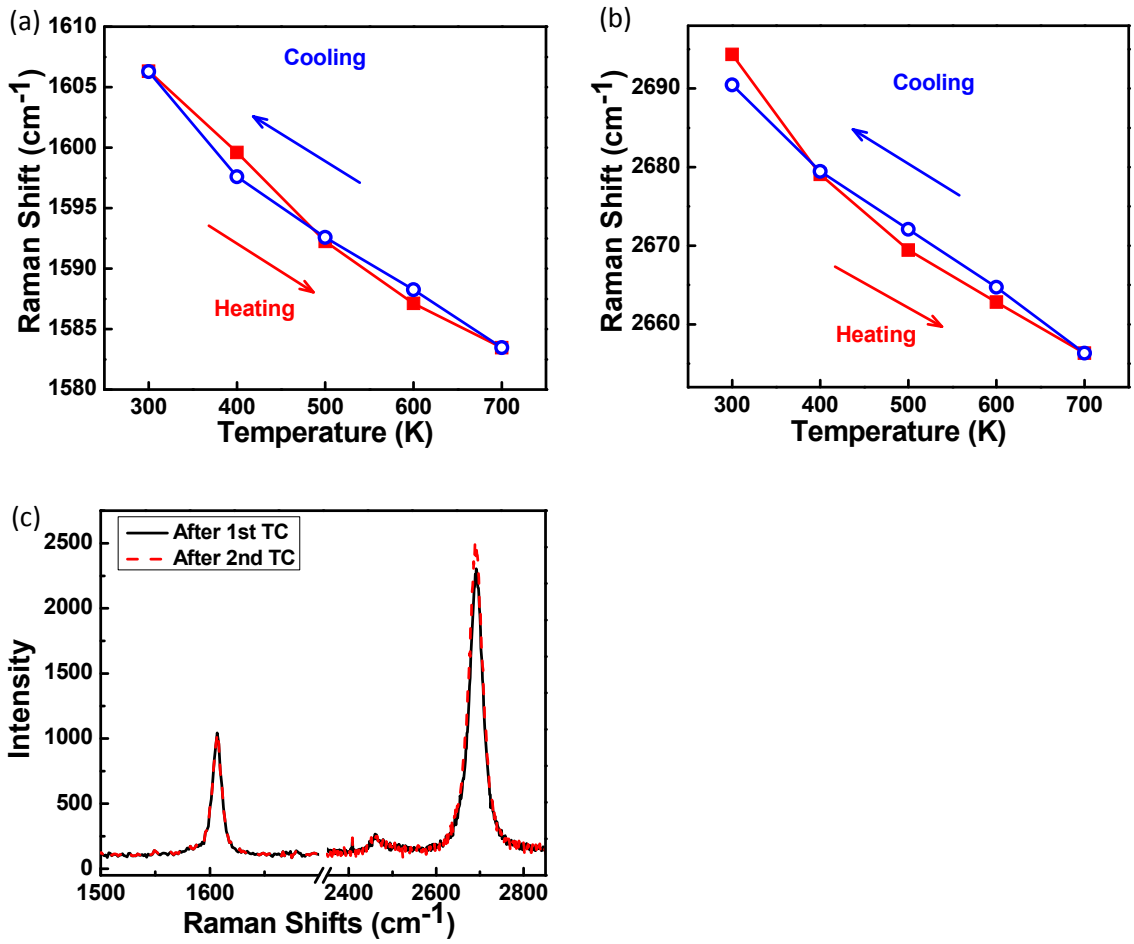

Figure 3. (a) *G* band and (b) *2D* band Raman data of single layer graphene taken during the second thermal cycling. (c) Raman spectrum before and after the second thermal cycling (TC).

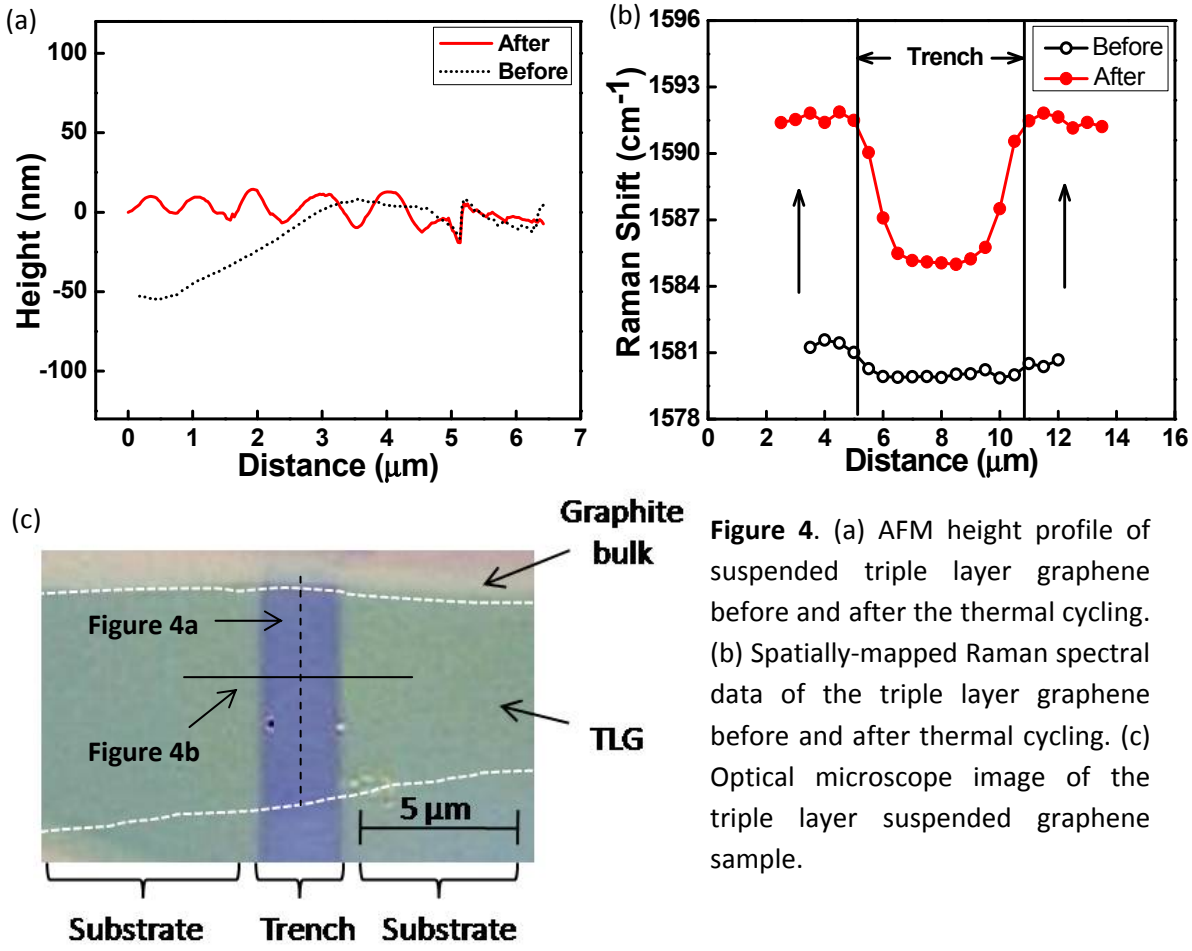

Figure 4. (a) AFM height profile of suspended triple layer graphene before and after the thermal cycling. (b) Spatially-mapped Raman spectral data of the triple layer graphene before and after thermal cycling. (c) Optical microscope image of the triple layer suspended graphene sample.

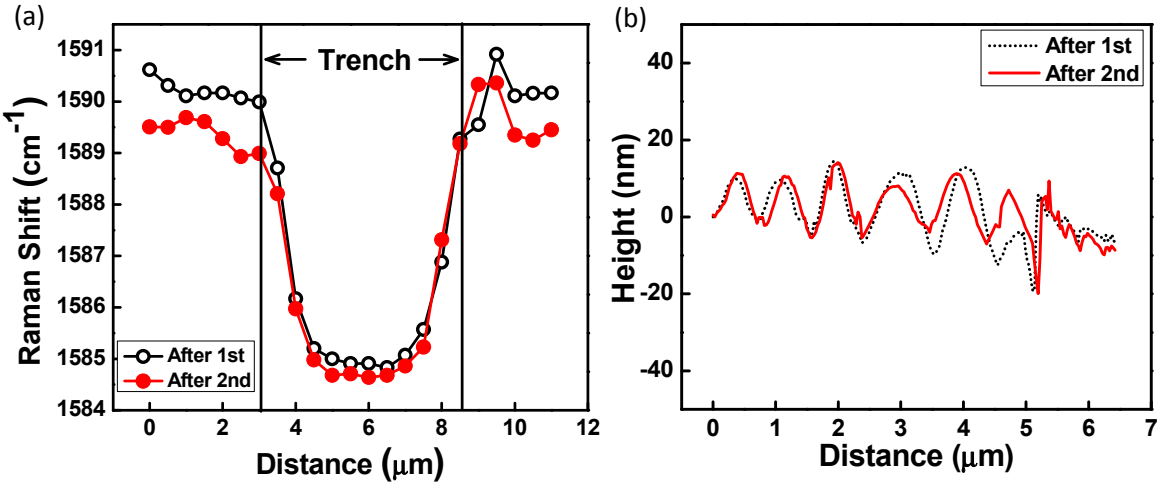

Figure 5. (a) Spatially-mapped Raman spectral data and (b) AFM height profile of the bilayer graphene show in Figure 4 before and after the second thermal cycling to 700K.

(a) (b)

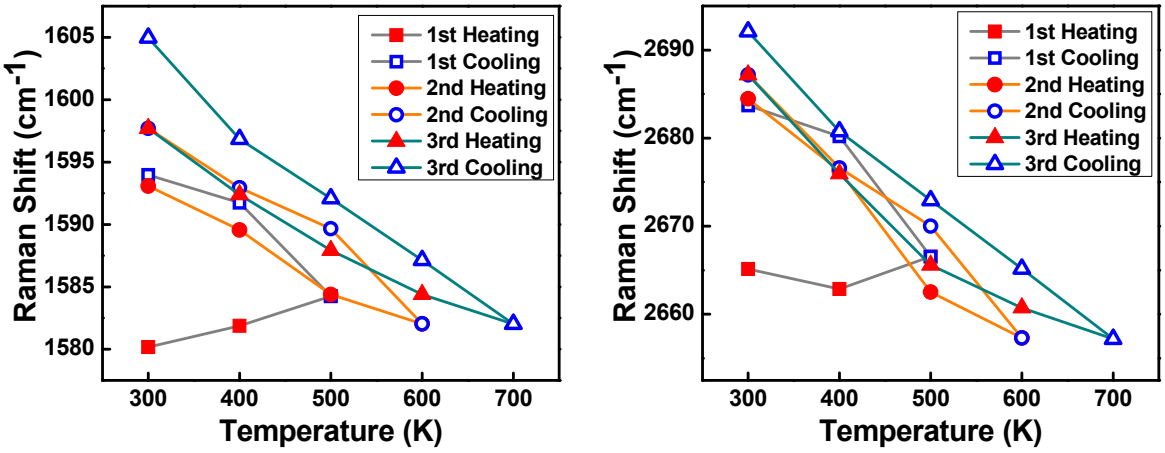

Figure 6. (a) *G* band and (b) *2D* band Raman data of single layer graphene taken during three thermal cycles to 500K, 600K, and 700K.

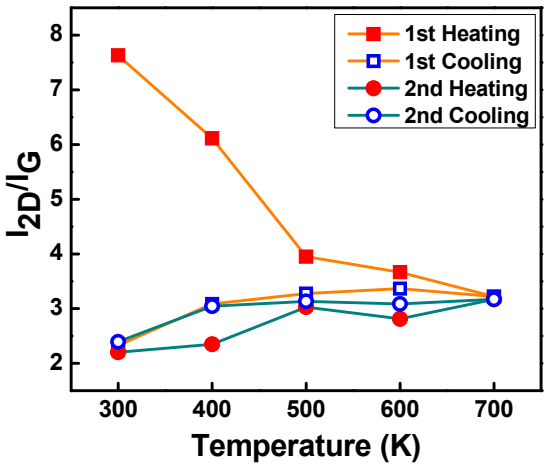

Figure 7. Raman intensity ratio of the *2D* and *G* bands taken during the first and second thermal cycles.

Sample	Changes in the Raman frequency after 700K thermal cycling (cm^{-1})				Gas	$\frac{\left(\frac{I_{2D}}{I_G}\right)_{Before} - \left(\frac{I_{2D}}{I_G}\right)_{After}}{\left(\frac{I_{2D}}{I_G}\right)_{Before}}$		Raman temperature coefficient (K^{-1})	
	G band		*2D* band						
	1st cycle	2nd cycle	1st cycle	2nd cycle		1st cycle	2nd cycle	$\partial\omega_G/\partial T$	$\partial\omega_{2D}/\partial T$
SLG1	**24.4**	**-0.03**	**23.2**	**-3.86**	**Air**	**0.69**	**-0.086**	**-0.055**	**-0.083**
SLG2	**24.8**	**NA**	**26.9**	**NA**	**Air**	**0.69**	**NA**	**-0.055**	**-0.085**
SLG3	**21.3**	**NA**	**27.2**	**NA**	**Ar**	**0.42**	**NA**	**-0.048**	**-0.080**

Table 1. Summary of Raman data taken on three different SLG samples after thermal cycling to 700K.